

Highly polarized Raman scattering anisotropy in single GaN nanowires

E. O. Schäfer-Nolte, T. Stoica, T. Gotschke, F. Limbach, E. Sutter, P. Sutter, and R. Calarco

Citation: [Applied Physics Letters](#) **96**, 091907 (2010); doi: 10.1063/1.3343347

View online: <http://dx.doi.org/10.1063/1.3343347>

View Table of Contents: <http://scitation.aip.org/content/aip/journal/apl/96/9?ver=pdfcov>

Published by the [AIP Publishing](#)

Articles you may be interested in

[Size and shape effects in the Raman scattering by single GaN nanowires](#)

J. Appl. Phys. **114**, 223506 (2013); 10.1063/1.4839975

[Blue single photon emission up to 200K from an InGaN quantum dot in AlGaN nanowire](#)

Appl. Phys. Lett. **102**, 161114 (2013); 10.1063/1.4803441

[Raman scattering of phonon-plasmon coupled modes in self-assembled GaN nanowires](#)

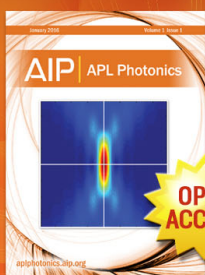
J. Appl. Phys. **105**, 123707 (2009); 10.1063/1.3148862

[Raman scattering study on anisotropic property of wurtzite GaN](#)

J. Appl. Phys. **105**, 036102 (2009); 10.1063/1.3072705

[Multiphonon Raman scattering in GaN nanowires](#)

Appl. Phys. Lett. **90**, 213104 (2007); 10.1063/1.2741410



Launching in 2016!

The future of applied photonics research is here

AIP | APL
Photonics

Highly polarized Raman scattering anisotropy in single GaN nanowires

E. O. Schäfer-Nolte,^{1,2} T. Stoica,^{1,a)} T. Gotschke,¹ F. Limbach,¹ E. Sutter,² P. Sutter,² and R. Calarco¹

¹*Institute of Bio- and Nanosystems (IBN-1), Research Centre Jülich GmbH and JARA-FIT (Fundamentals of Future Information Technology), 52425 Jülich, Germany*

²*Center for Functional Nanomaterials, Brookhaven National Laboratory, Upton, New York 11973, USA*

(Received 22 January 2010; accepted 10 February 2010; published online 3 March 2010)

Single GaN nanowires and larger GaN ensembles are investigated by Raman spectroscopy. Spectra of nanowire ensembles prove the high crystal quality and are in agreement with selection rules for the wurtzite structure. Single nanowires are studied with a spatial resolution of the order of 400 nm for different polarization directions of the incident laser beam relative to the nanowire axis. In the single wire spectrum, only the $A_1(\text{TO})$ was observed and the Raman intensity was suppressed for perpendicular polarization. These results confirm that Raman scattering in isolated GaN nanowires is governed by size effects. © 2010 American Institute of Physics. [doi:10.1063/1.3343347]

Gallium nitride is a promising semiconductor material due to its wide direct band gap, large breakdown field, high carrier mobility, and thermal stability.¹ These properties make the material ideally suited for short-wavelength optoelectronic devices such as light emitting and laser diodes,^{2–4} as well as for high-power and high-temperature electronics.^{5,6} GaN nanowires feature a low density of structural defects^{7,8} and are therefore possible building blocks for future nanoelectronic devices.⁹

Important for the performance of such devices are both the crystalline as well as the electronic properties of the nanowires. The combination of confocal microscopy and Raman spectroscopy offers in principle the possibility to investigate these properties with a spatial resolution of roughly half the excitation wavelength. Due to the well-defined scattering geometry, Raman spectroscopy on single wires allows furthermore to study the phonon symmetries and how they are affected by the finite size of the crystal.

The first-order phonon Raman scattering for bulk GaN follows the selection rules corresponding to its wurtzite structure.¹⁰ A first study on polarized Raman scattering of single GaN nanowires was published by Pauzauskie *et al.*¹¹ They observed $A_1(\text{LO})$ and E_2^{H} Raman modes in all spectra but with intensities which depend on the laser polarization plane with respect to the nanowire axis. Livneh *et al.*¹² performed a detailed study of phonon symmetries in GaN nanowires. They found the Raman intensities to be determined by the symmetry of complex-valued Raman tensors of the individual bands. An effect of the finite crystal size was not observed in their measurements. In the studies reported in Refs. 11 and 12, the nanowires were obtained by vapor-liquid-solid synthesis with diameters larger than 150 nm. In contrast to these results, in our study we analyzed nanowires (NWs) grown by catalyst-free plasma assisted molecular beam epitaxy (PAMBE) with diameter smaller than 100 nm, and highly polarized Raman scattering was observed, as discussed below.

For a cylindrical nanowire with a diameter much smaller than the wavelength of the excitation light, one can show that the internal field polarized perpendicular to the nanowire axis is attenuated with respect to the external field. An elec-

trostatic approximation results in a damping factor between parallel and perpendicular electric field of $2\varepsilon_0/(\varepsilon + \varepsilon_0)$, where ε and ε_0 are the dielectric constant of the GaN and surrounding medium, respectively.^{13,14} If only this dielectric shape effect is taken into consideration, the resulting attenuation factor for GaN NWs should be of the order of 30%. This shape effect overcomes the selection rules for Raman scattering resulting from tensor symmetry, and scattering modes can be suppressed due to this anisotropy. Raman studies on CuO (Ref. 15) and CdS (Ref. 16) nanowires with average diameters around 65 nm have shown that the intensities of all Raman modes (except E_2^{H} of the CdS nanowire in Ref. 16) showed a $\cos^2 \Theta$ dependence, where Θ is the angle between the laser polarization and the nanowire axis. This means that the Raman scattering was strongly suppressed if the excitation light was polarized perpendicular to the nanowire axis. A similar polarization dependency was also found in photoluminescence measurements on nanowires of different materials, such as InP,¹⁴ Si,¹⁷ and CdSe.¹⁸

In this work we present results from Raman spectroscopy studies on single GaN nanowires with an average diameter of 70 nm, which exhibit a strong dependency of the scattering intensity on the polarization direction of the excitation light.

The nanowires were grown catalyst-free by PAMBE on Si(111) substrates. Details of the growth mechanism as well as optical and electrical characterization have been discussed elsewhere.^{7,8,19–30} The nanowires are single crystalline, 50–90 nm in diameter and up to 2 μm in length. Raman spectra of the as grown samples, i.e., ensembles of GaN NWs, were measured in backscattering geometry using a laser wavelength of 514 nm and an excitation power of 25 mW. The laser beam was focused through a microscope (100 \times , NA 0.9) to a spot size $<2 \mu\text{m}$ in diameter. The spectra were measured with a resolution of 0.8 cm^{-1} using a 1800 grooves/mm grating spectrometer. Additionally, individual nanowires were removed from the growth substrate and transferred by a dry method to a graphite crystal (highly ordered pyrolytic graphite). On such samples Raman scattering measurements were carried out using a WITec alpha300 microscopy system with a 532 nm laser as excitation source. A 100 \times microscope objective (NA 0.9) was used to focus the laser beam to a spot size of about 400 nm, the excitation power on the sample was reduced to 5 mW to avoid laser

^{a)}Electronic mail: t.stoica@fz-juelich.de.

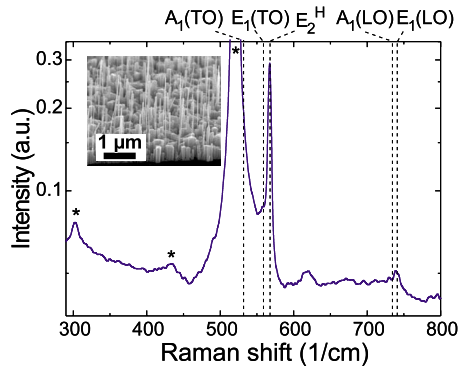


FIG. 1. (Color online) Raman spectrum of a GaN nanowire ensemble measured with 514 nm excitation wavelength. Black dotted lines show Raman mode frequencies reported in the literature (Ref. 10). The asterisks mark Raman modes of the silicon substrate. Inset is a SEM image of the as grown NW sample.

heating effects. The scattered light was analyzed using a 600 grooves/mm grating spectrometer with a spectral resolution of about 3 cm^{-1} . Spatially resolved intensity maps are obtained by scanning the sample relative to the laser beam with a piezoelectrical stage. Since the Raman signal of a single GaN nanowire is very weak, the wire was imaged by mapping the intensity of the E_{2g} Raman mode of the graphite substrate. It was observed that this intensity is strongly enhanced when the wire is in the laser focus. Therefore a good contrast between the nanowire and the graphite substrate could be reached in a relative short acquisition time (about 20 min for a complete map). The laser spot was subsequently positioned on the localized wire and a single spectrum with an integration time of 1 h was recorded.

A typical Raman spectrum of an as grown ensemble of GaN nanowires is shown in Fig. 1. Since the nanowires grow predominantly perpendicular to the silicon substrate, the nanowire axis, i.e., the crystal c -axis,³⁰ is oriented parallel to the incident laser beam. In this $z(-,-)\bar{z}$ geometry with z parallel to the c -axis, the selection rules for the wurtzite structure predict the appearance of E_2^H and $A_1(LO)$ Raman lines. Besides the first and second order Raman modes from the silicon substrate, marked by asterisks in Fig. 1, the spectrum exhibits a strong E_2^H Raman mode at 568 cm^{-1} . The small value of the full width at half maximum (FWHM) of about 3.5 cm^{-1} proves the high crystal quality of the nanowires. A second peak can be found at 739 cm^{-1} close to the expected position of the longitudinal-optical (LO) modes. The deviation of this peak from the expected 734 cm^{-1} value for $A_1(LO)$ of the bulk GaN is probably due to coupling of the LO phonon to plasmons.³¹

The Raman spectra of single nanowires differ considerably from spectrum of the ensemble. Spectra of two wires with different diameters are shown in Fig. 2 together with scanning electron microscopy (SEM) micrographs of the corresponding nanowires. Since the nanowire axis is perpendicular to the incident laser beam, the scattering configuration is denoted by $x(-,-)\bar{x}$. In this geometry $A_1(TO)$, $E_1(TO)$, and E_2^H are symmetry-allowed modes but only $A_1(TO)$ is clearly expressed in the spectra of Fig. 2. Wire A, 2 μm long and $55\text{--}65 \text{ nm}$ in diameter, shows the $A_1(TO)$ peak at 536.8 cm^{-1} with a line width of about 12 cm^{-1} . For wire B, 1.2 μm in length and 70 nm in diameter, the $A_1(TO)$ mode has a Raman shift of 535.3 cm^{-1} and a full-width at half

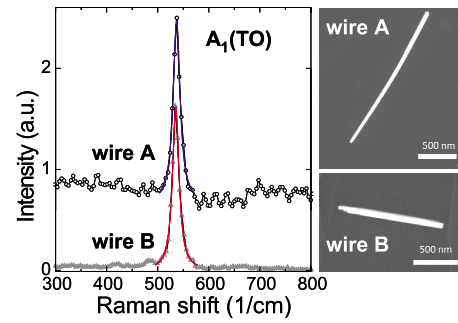


FIG. 2. (Color online) Raman spectra of single GaN nanowires measured in $x(-,-)\bar{x}$ geometry. On the right, SEM micrographs of the corresponding nanowires.

maximum (FWHM) of about 15 cm^{-1} . We attribute the fluctuations in the Raman mode frequency and FWHM to the relatively low spectral resolution and to different sample temperatures arising from fluctuations from wire to wire in the thermal contact between nanowire and substrate. For the diameters of the nanowires studied in these measurements, phonon confinement effects are not expected.^{32,33}

The absence of E_2^H and $E_1(TO)$ in the spectra measured in $x(-,-)\bar{x}$ geometry is in contrast to the results on bulk GaN (Refs. 10 and 34) and thick GaN nanowires^{11,12} published so far. For a better understanding of the peculiarity of the single wire spectra we investigated their dependency on the polarization of the excitation light, by rotating the sample while keeping the laser polarization fixed. A typical result is shown in Fig. 3. The orientation of the nanowire with respect to the laser polarization can be seen for the different measurements in the Raman maps shown as insets in Fig. 3. Raman spectra were recorded at different positions on the nanowire, denoted by A–D in the maps. If the nanowire is oriented parallel to the laser polarization, the Raman spectra exhibit a pronounced $A_1(TO)$ mode. The scattering configuration in this geometry is $x(z,-)\bar{x}$, which allows the $A_1(TO)$ and $E_1(TO)$ modes. If the nanowire is oriented perpendicular to the polarization, which corresponds to a $x(y,-)\bar{x}$ scattering configuration, the scattering intensity almost vanishes, although selection rules allow E_2^H , $A_1(TO)$, and $E_1(TO)$. As can be

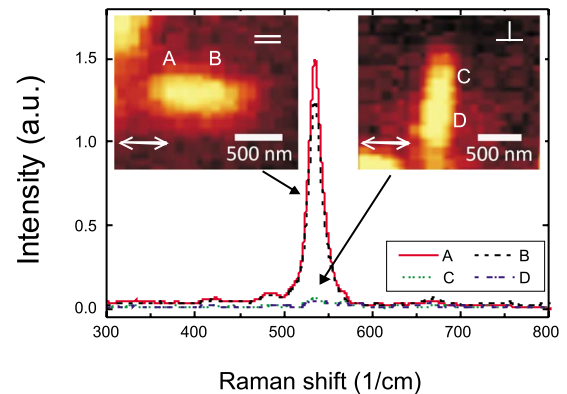


FIG. 3. (Color online) Raman spectra of the same GaN nanowire for different orientations of the nanowire axis with respect to the polarization of the excitation light. Insets show Raman images of the two used geometries obtained by mapping the intensity of the E_{2g} band of the graphite substrate (the lateral resolution is low and therefore the images can be used only to probe the wire orientation). The white arrows illustrate the polarization of the incident light. For each wire two measurements were performed. A–D mark the region where the corresponding spectra were measured.

seen in Fig. 3, the contrast in the Raman map of the graphite signal is not affected by the nanowire orientation. The observed polarization dependence indicates that the Raman spectra are governed by the nanowire shape rather than by the selection rules of the wurtzite structure. If one assumes that the perpendicular field component is strongly reduced inside the nanowire due to the dielectric shape effect, the E_2^H mode, which arises only in $x(y, y)\bar{x}$ scattering with laser polarization normal to the wire, cannot be excited. The same effect would prevent the observation of $E_1(\text{TO})$ arising from $x(y, z)\bar{x}$ scattering. The attenuation of the internal field would thus explain the suppressed Raman scattering in the case of a perpendicular orientation of the nanowire with respect to the laser polarization. The observed polarization anisotropy is much stronger than expected if the simple dielectric cylinder model from Ref. 14 is taken into account. This might be a consequence of the electrostatic approximation employed in this model. Additionally the anisotropy could be enhanced by a proximity effect of the graphite substrate and therefore future investigations are planned to clarify this aspect.

Thus the question arises why a strong E_2^H mode was observed in the Raman spectrum of GaN nanowire ensembles (Fig. 1) while it was not detected in individual nanowire measurements. One possibility is that it is related to the morphology of the GaN ensembles. In the as-grown samples there is a high density of thin and thick NWs close to the substrate and the ensemble behaves like an effective medium of NWs and voids in which the incident light is inserted into the wires through the top facets and propagates parallel to the c -axis, giving rise to E_2^H scattering in $z(-, -)\bar{z}$ geometry.

In conclusion, Raman scattering experiments have been performed on undoped GaN nanowire ensembles as well as individual nanowires. The spectra from the nanowire ensembles did not reveal a deviation from the selection rules for the wurtzite structure. In the single NW spectra, only $A_1(\text{TO})$ was observed, with suppressed intensity for laser polarization perpendicular to the nanowire axis. These results indicate that Raman scattering in isolated GaN nanowires thinner than 100 nm is governed by size effects, which modify the selection rules for the bulk crystal.

The authors gratefully acknowledge fruitful discussions and suggestions by Professor D. Grützmacher. The authors wish to thank also K. H. Deussen for technical support. This work was financially supported by the German Ministry of Education and Research project "QPENS." It was performed in part under the auspices of the U.S. Department of Energy, under Contract No. DE-AC02-98CH1-886.

¹S. C. Jain, M. Willander, J. Narayan, and R. Van Overstraeten, *J. Appl. Phys.* **87**, 965 (2000).

²M. R. Krames, O. B. Shchekin, R. Mueller-Mach, G. O. Mueller, L. Zhou,

G. Harbers, and M. G. Craford, *J. Disp. Technol.* **3**, 160 (2007).

³S. Nakamura, *MRS Bull.* **34**, 101 (2009).

⁴J. Edmond, A. Abare, M. Bergman, J. Bharathan, K. L. Bunker, D. Emerson, K. Haberern, J. Ibbetson, M. Leung, P. Russel, and D. Slater, *J. Cryst. Growth* **272**, 242 (2004).

⁵N. Defrance, V. Hoel, Y. Douvry, J. C. De Jaeger, C. Gaquiere, X. Tang, M. Rousseau, M. A. di Forte-Poisson, J. Thorpe, H. Lahrech, and R. Langer, *IEEE Electron Device Lett.* **30**, 596 (2009).

⁶S. Arulkumaran, G. I. Ng, Z. H. Liu, and C. H. Lee, *Appl. Phys. Lett.* **91**, 083516 (2007).

⁷R. Calarco, R. Meijers, R. K. Debnath, T. Stoica, E. Sutter, and H. Lüth, *Nano Lett.* **7**, 2248 (2007).

⁸R. Meijers, T. Richter, R. Calarco, T. Stoica, H.-P. Bochem, M. Marso, and H. Lüth, *J. Cryst. Growth* **289**, 381 (2006).

⁹C. M. Lieber and Z. L. Wang, *MRS Bull.* **32**, 99 (2007).

¹⁰H. Harima, *J. Phys.: Condens. Matter* **14**, R967 (2002).

¹¹P. J. Pauzauskie, D. Talaga, K. Seo, P. Yang, and F. Lagugné-Labarhet, *J. Am. Chem. Soc.* **127**, 17146 (2005).

¹²T. Livneh, J. Zhang, G. Cheng, and M. Moskovits, *Phys. Rev. B* **74**, 035320 (2006).

¹³L. D. Landau, E. M. Lifschitz, and L. P. Pitaevskii, *Electrodynamics of Continuous Media* (Pergamon, Oxford, 1984), pp. 34–42.

¹⁴J. Wang, M. S. Gudiksen, X. Duan, Y. Cui, and C. M. Lieber, *Science* **293**, 1455 (2001).

¹⁵T. Yu, X. Zhao, Z. X. Shen, Y. H. Wu, and W. H. Su, *J. Cryst. Growth* **268**, 590 (2004).

¹⁶H. M. Fan, X. F. Fan, Z. H. Ni, Z. X. Shen, Y. P. Feng, and B. S. Zou, *J. Phys. Chem. C* **112**, 1865 (2008).

¹⁷J. Qi, A. M. Belcher, and J. M. White, *Appl. Phys. Lett.* **82**, 2616 (2003).

¹⁸C. X. Shan, Z. Liu, and S. K. Hark, *Phys. Rev. B* **74**, 153402 (2006).

¹⁹R. K. Debnath, R. Meijers, T. Richter, T. Stoica, R. Calarco, and H. Lüth, *Appl. Phys. Lett.* **90**, 123117 (2007).

²⁰T. Richter, H. Lüth, R. Meijers, R. Calarco, and M. Marso, *Nano Lett.* **8**, 3056 (2008).

²¹J. Ebbecke, S. Maisch, A. Wixforth, R. Calarco, R. Meijers, M. Marso, and H. Lüth, *Nanotechnology* **19**, 275708 (2008).

²²L. Polenta, A. Cavallini, M. Rossi, R. Calarco, M. Marso, T. Stoica, R. Meijers, T. Richter, and H. Lüth, *ACS Nano* **2**, 287 (2008).

²³A. Cavallini, L. Polenta, M. Rossi, T. Stoica, R. Calarco, R. J. Meijers, T. Richter, and H. Lüth, *Nano Lett.* **7**, 2166 (2007).

²⁴R. Calarco and M. Marso, *Appl. Phys. A: Mater. Sci. Process.* **87**, 499 (2007).

²⁵A. Cavallini, L. Polenta, M. Rossi, T. Richter, M. Marso, R. Meijers, R. Calarco, and H. Lüth, *Nano Lett.* **6**, 1548 (2006).

²⁶A. G. Milekhin, R. Meijers, T. Richter, R. Calarco, S. Montanari, H. Lüth, B. A. Paez Sierra, and D. R. T. Zahn, *J. Phys.: Condens. Matter* **18**, 5825 (2006).

²⁷A. G. Milekhin, R. Meijers, T. Richter, R. Calarco, H. Lüth, and D. R. T. Zahn, *Phys. Status Solidi C* **3**, 2065 (2006).

²⁸N. Thillosen, K. Sebald, H. Hardtdegen, R. Meijers, R. Calarco, S. Montanari, N. Kaluza, J. Gutowski, and H. Lüth, *Nano Lett.* **6**, 704 (2006).

²⁹R. Calarco, M. Marso, T. Richter, A. I. Aykanat, R. Meijers, A. d. Hart, T. Stoica, and H. Lüth, *Nano Lett.* **5**, 981 (2005).

³⁰T. Stoica, E. Sutter, R. Meijers, R. K. Debnath, R. Calarco, and H. Lüth, *Small* **4**, 751 (2008).

³¹K. Jeganathan, R. K. Debnath, R. Meijers, T. Stoica, R. Calarco, D. Grützmacher, and H. Lüth, *J. Appl. Phys.* **105**, 123707 (2009).

³²H.-L. Liu, C.-C. Chen, C.-T. Chia, C.-C. Yeh, C.-H. Chen, M.-Y. Yu, S. Keller, and S. P. Den Baars, *Chem. Phys. Lett.* **345**, 245 (2001).

³³L. Zhang and J.-J. Shi, *Appl. Surf. Sci.* **252**, 7815 (2006).

³⁴H. C. Lin, Z. C. Feng, M. S. Chen, Z. X. Shen, I. T. Ferguson, and W. Lu, *J. Appl. Phys.* **105**, 036102 (2009).